

Short Communication

Potentiodynamic Deposition of Cu Doped $\text{Bi}_x\text{Cu}_y\text{Sb}_{2-x-y}\text{Te}_z$ Thin Film as Thermoelectric Materials

Feihui Li¹, Gao Jinghan¹, Wei Wang², Yunlan Gong^{1,*}

¹ Department of Applied Chemistry, School of Biotechnology and Food Science, Tianjin University of Commerce, Tianjin 300134, P R China;

² School of Chemical Engineering & Technology, Tianjin University, Tianjin 300072, P R China

*E-mail: tjcugyl@126.com

Received: 2 July 2022 / Accepted: 22 August 2022 / Published: 10 September 2022

In this paper, the preparation of Cu-doped $\text{Bi}_x\text{Cu}_y\text{Sb}_{2-x-y}\text{Te}_z$ thin film thermoelectric materials by electrodeposition in inorganic solution system was studied. The effects of Cu^{2+} concentration on the properties of $\text{Bi}_x\text{Cu}_y\text{Sb}_{2-x-y}\text{Te}_z$ thin film thermoelectric materials were investigated. The composition, morphology and phase of the prepared $\text{Bi}_x\text{Cu}_y\text{Sb}_{2-x-y}\text{Te}_z$ thin films were characterized by energy dispersive spectroscopy, environmental scanning electron microscope and X-ray diffraction. The conductivity and Seebeck coefficient of $\text{Bi}_x\text{Cu}_y\text{Sb}_{2-x-y}\text{Te}_z$ thin film prepared under different conditions were also tested. The results show that doping of Cu element into $\text{Bi}_x\text{Sb}_{2-x}\text{Te}_z$ thermoelectric material can not only reduce the resistivity of the material, but also improve the morphology of the material, and the Seebeck coefficient of $\text{Bi}_x\text{Cu}_y\text{Sb}_{2-x-y}\text{Te}_z$ thermoelectric material can reach up to 152 $\mu\text{V}/\text{K}$. When the Cu^{2+} concentration is 1.28 mmol L^{-1} , the highest power factor of 577.6 $\mu\text{W}\cdot\text{K}^{-2}\cdot\text{m}^{-1}$ can be obtained.

Keywords: potentiodynamic deposition; Cu-doped; $\text{Bi}_x\text{Cu}_y\text{Sb}_{2-x-y}\text{Te}_z$ films; thermoelectric performance

1. INTRODUCTION

In the 21st century, with the increasingly serious world environmental pollution and energy crisis, the development of renewable green energy has received more and more attention [1]. The concepts of green development and sustainable development have become the consensus of mankind, therefore, countries all around the world are actively combining the development of new materials with green development, and vigorously promoting the development and application of new energy and environmental materials closely related to green development.

Thermoelectric materials can realize the direct conversion of thermal energy to electric energy,

so they have important application potential in the field of energy and now have attracted a lot of scientific research attentions. Thermoelectric devices based on thermoelectric materials can generate electricity using various forms of heat, such as radiant heat, solar heat, body heat, geothermal heat and various waste heats [2-5], and their energy conversion performance can usually be characterized by dimensionless thermoelectric merit ZT .

$$ZT = S^2\sigma T/\kappa$$

Where, S is Seebeck coefficient, σ is conductivity, T is absolute temperature, κ is thermal conductivity and $S^2\sigma$ is power factor. Therefore, there are two ways to improve the performance of thermoelectric materials, namely, reducing the κ or increasing the power factor.

In recent years, researchers have made a lot of progress in the development and optimization of various thermoelectric materials, among which Bi_2Te_3 based alloys have the best performance around room temperature [6-10]. With the growth of miniaturized generator parts market, the research on Bi_2Te_3 based thin film thermoelectric materials has also attracted more and more attentions. The key to improve the properties of thin film thermoelectric materials is to optimize the alloy composition and microstructure. Reasonable alloy element composition can be used to adjust the carrier concentration and electron band structure, so as to improve the Seebeck coefficient of the material [11-12]. It has been reported that in the bulk $\text{Bi}_{1-x}\text{Sb}_x\text{Te}_3$ thermoelectric material prepared by physical method, doping trace Cu can greatly reduce the resistivity of the material [13-14].

At present, there are many technologies that can be used to prepare Bi_2Te_3 based thin film thermoelectric materials, such as chemical vapor deposition (CVD) [15], molecular beam epitaxy (MBE)[16,17], pulsed laser deposition (PLD) [18,19], thermal evaporation[20], magnetron sputtering[21], electrochemical deposition[22-24] and so on. However, compared with other physical and chemical preparation methods, electrochemical deposition has many advantages, such as mild preparation conditions, simple equipment, low cost and easy operation [25]. Therefore, electrodeposition technology is widely used in the preparation of thin film thermoelectric materials.

The electrodeposition modes used in the reported literature mainly include potentiostatic deposition, galvanostatic deposition and pulse electrodeposition. Marisol [26] successfully prepared $\text{Bi}_{0.5}\text{Sb}_{1.5}\text{Te}_3$ thin films and nanowire materials by cathodic potentiostatic co-deposition technology. Boulanger [27] optimized the deposition conditions of Bi-Sb-Te alloy by comparing the electrochemical behavior of Bi-Te system and Sb-Te system. They also used pulse electrodeposition to reduce the roughness of $(\text{Bi}_{0.25}\text{Sb}_{0.75})_2\text{Te}_3$ thermoelectric thin films prepared by electrodeposition, and found that the Seebeck coefficient and resistivity of the deposited thermoelectric thin films were greatly related to the cathode pulse current density and film thickness [28]. In addition, they also studied the effects of pulse parameters on the morphology, composition, thermoelectric properties and nucleation mechanism of Bi-Te alloy films prepared by pulse electrodeposition [29-30]. Yoon [31] proposed a process for preparing $(\text{Bi,Sb})_2\text{Te}_3$ thin film thermoelectric material by constant current deposition. $(\text{Bi,Sb})_2\text{Te}_3$ thin film material with power factor equivalent to that prepared by magnetron sputtering can be obtained by this process. However, these electrodeposition modes have some limitations. It is difficult to obtain thick film thermoelectric materials with good morphology and high thermoelectric properties by using these current electrodeposition modes. Therefore, it is necessary to try new electrodeposition methods.

At present, there are few reports on the doping of copper element in bismuth telluride based thin film thermoelectric materials by electrochemical methods and the influence of copper element content on the properties of materials. And there are no reports on the preparation of such materials using the potentiodynamic deposition mode. Therefore, in this paper, potentiodynamic deposition was proposed to prepare Cu doped $\text{Bi}_x\text{Cu}_y\text{Sb}_{2-x-y}\text{Te}_z$ thin film thermoelectric materials. And the effects of Cu^{2+} ion concentration on the morphology, composition and thermoelectric properties of $\text{Bi}_x\text{Cu}_y\text{Sb}_{2-x-y}\text{Te}_z$ thermoelectric thin film materials prepared by potentiodynamic deposition were studied.

2. EXPERIMENTAL

Bismuth nitrate pentahydrate ($\text{Bi}(\text{NO}_3)_3 \cdot 5\text{H}_2\text{O}$) and nitric acid (HNO_3) were obtained from Tianjin Chemical Reagent Co. Potassium nitrate (KNO_3), tartaric acid ($\text{C}_4\text{H}_6\text{O}_6$) and copper sulfate pentahydrate ($\text{CuSO}_4 \cdot 5\text{H}_2\text{O}$) were bought from Sinopharm Chemical Reagent Co., Ltd. Antimony trioxide (Sb_2O_3) and potassium tellurite (K_2TeO_3) were purchased from Tianjin Guangfu Fine Chemical Research Institute. All chemicals are analytical grade and used as received.

The preparation method of electrolyte is as follows: firstly, dissolve a certain amount of $\text{Bi}(\text{NO}_3)_3 \cdot 5\text{H}_2\text{O}$ and K_2TeO_3 in concentrated nitric acid aqueous solution, and then dissolve Sb_2O_3 (analytical reagent) in concentrated tartaric acid solution at $80\text{ }^\circ\text{C}$, then mix the above two solutions. Subsequently, KNO_3 and different amount of $\text{CuSO}_4 \cdot 5\text{H}_2\text{O}$ were added to the mixed solution and dissolved. And finally, the solution is diluted to the required concentration with deionized water (as shown in Tab.1).

Table 1. Composition of the electrolytes for all systems

Component	Concentration
$c(\text{Bi}(\text{NO}_3)_3 \cdot 5\text{H}_2\text{O}) / (\text{mmol L}^{-1})$	4
$c(\text{K}_2\text{TeO}_3) / (\text{mmol L}^{-1})$	6
$c(\text{Sb}_2\text{O}_3) / (\text{mmol L}^{-1})$	10
$c(\text{C}_4\text{H}_6\text{O}_6) / (\text{mol L}^{-1})$	0.67
$c(\text{HNO}_3) / (\text{mol L}^{-1})$	1
$c(\text{KNO}_3) / (\text{g L}^{-1})$	50
$c(\text{CuSO}_4 \cdot 5\text{H}_2\text{O}) / (\text{mmol L}^{-1})$	0 ~7.65

The electrodeposition was carried out using CHI660B electrochemical workstation and a standard three-electrode cell at $25 \pm 1\text{ }^\circ\text{C}$. An Au sheet electrode (1 cm^2), a Pt sheet electrode (2 cm^2) and a saturated calomel electrode (SCE) were used as the working electrode, auxiliary electrode and the reference electrode, respectively. The salt bridge was made of saturated potassium nitrate and agar. All the potentials listed in this paper were expressed related to the saturated calomel electrode. The thin film materials were prepared by potentiodynamic deposition mode. Actually, this deposition mode is to use the cyclic voltammetry technology, select the appropriate potential scanning range, and realize

the deposition of materials through multiple cycles of potential. The potentiodynamic deposition parameters are determined as follows: potential scanning range is 20 mV to -200 mV, the potential scan rate is 20 mV/s, the electric quantity of electrodeposition is 15 C/cm^2 , and the coating thickness is about $15\text{ }\mu\text{m}$. The prepared thin films were annealed at $200\text{ }^\circ\text{C}$ in nitrogen atmosphere for 2 h.

The Seebeck coefficient and resistivity of the thin films were measured by a Seebeck coefficient test system (TDS1-2) and a four probe thin film thermoelectric material resistivity measurement system (TDR2-3) developed by Tianjin University, respectively. The elemental composition of electrodeposited thin film was detected by OXFORD-ISIS300 energy dispersive spectrometer (EDS). XL30ESEM TMP environmental scanning electron microscope (ESEM, Philips Company in the UK) was used to analyze the micro-morphology of the prepared film materials. The phase analysis was carried out by Rigaku D/max 2500v/pc X-ray diffractometer (XRD) using $\text{CuK}\alpha$ radiation. The tube pressure of the X-ray diffractometer is 40 kV, the tube flow is 200 mA, and the scanning rate is $4^\circ/\text{min}$.

3. RESULTS

3.1 Analysis of the potentiodynamic deposition process

Fig.1 shows the potentiodynamic curves for the $\text{Bi}_x\text{Cu}_y\text{Sb}_{2-x-y}\text{Te}_z$ thin film thermoelectric material deposition in the solution without Cu^{2+} . In the selected potential range of potentiodynamic scanning, two reduction peaks can be obviously observed, while no oxidation peak can be detected. It reveals that only the reduction reaction occurs in this potential range. According to the cyclic voltammetry curve test results obtained in our previous research [32], these reduction peaks are corresponding to the multi-step reduction process to form Bi-Sb-Te ternary compounds.

Unlike the traditional potentiostatic or galvanostatic electrodeposition, the potential changes rapidly, dynamically and cyclically in a much wider range when the materials are prepared by potentiostatic scanning. When the potential is positive, the deposition rate is slow, which is conducive to the diffusion and replenishment of ions in the solution and reduces the concentration polarization. When the potential is negative, it is beneficial to increase the electrochemical polarization, improve the electrocrystallization condition and promote the formation of multiple component compounds. However, in potentiostatic or galvanostatic electrodeposition, the potential or the current is always fixed at a certain value throughout the whole electrodeposition process, so it is difficult to have both of the above advantages.

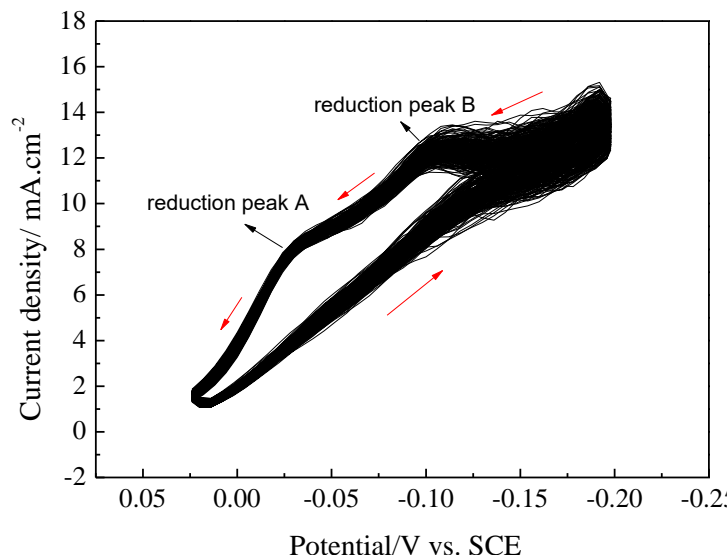


Figure 1. Potentiodynamic curves for the $\text{Bi}_x\text{Cu}_y\text{Sb}_{2-x-y}\text{Te}_z$ thin film thermoelectric material deposition

3.2 Effect of Cu^{2+} ion concentration on the composition of $\text{Bi}_x\text{Cu}_y\text{Sb}_{2-x-y}\text{Te}_z$ thin film thermoelectric materials

The composition of $\text{Bi}_x\text{Cu}_y\text{Sb}_{2-x-y}\text{Te}_z$ thin film thermoelectric materials prepared in the electrolyte with different Cu^{2+} ion concentration is shown in Fig.2. It can be seen that when the Cu^{2+} concentration in the electrolyte is lower than 5 mmol/L, the content of Sb element in the film material decreases significantly with the increase of Cu^{2+} concentration, and then remains basically unchanged. However, the change of Cu content in the material is just opposite to that of Sb. When the Cu^{2+} concentration is lower than 5 mmol/L, it increases significantly with the increase of Cu^{2+} concentration, and then remains basically unchanged. It indicates that with the increase of Cu^{2+} concentration in the solution, the proportion of Cu element replacing Sb element is also increasing. The content of Bi and Te element in the material changes little with the concentration of Cu^{2+} .

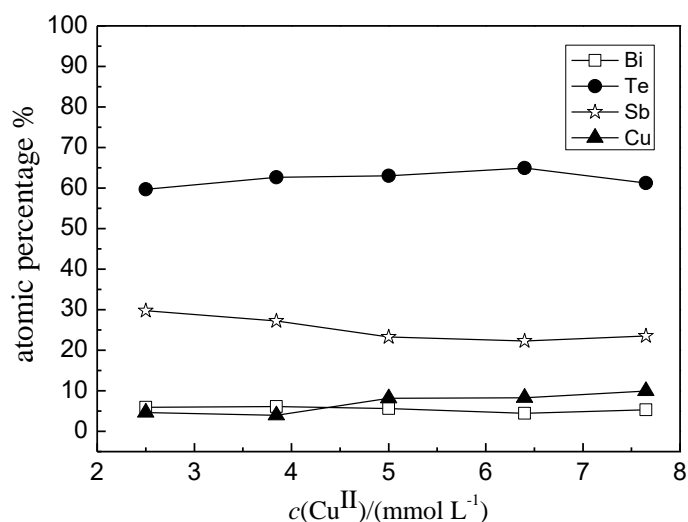


Figure 2. Relationship between Cu^{2+} concentration in the electrolyte and the atomic ratio of elemental Bi, Sb, Te and Cu in the thermoelectric film

3.3 Effect of Cu^{2+} ion concentration on the thermoelectric performance and structure of $\text{Bi}_x\text{Cu}_y\text{Sb}_{2-x-y}\text{Te}_z$ thin film thermoelectric materials

The resistivity, electrical conductivity, Seebeck coefficient and power factor of $\text{Bi}_x\text{Cu}_y\text{Sb}_{2-x-y}\text{Te}_z$ thin film thermoelectric materials prepared in the electrolyte containing different concentration of Cu^{2+} are listed in Tab.2. It can be seen that the electrical conductivity of the materials gradually increases with the increase of Cu^{2+} concentration, while the Seebeck coefficient first increases then decreases. Compared with the material without Cu element doped, the conductivity of the material is significantly increased after doping Cu element, while the Seebeck coefficient has little change. In particular, when the Cu^{2+} concentration is 1.28 mmol L^{-1} , not only the conductivity, the Seebeck coefficient of the material is also increased after doping Cu element and the highest power factor of $577.6 \mu\text{W}\cdot\text{K}^{-2}\cdot\text{m}^{-1}$ can be obtained.

Table 2. Relations between Cu^{2+} concentration in the electrolyte and thermoelectric properties of the thermoelectric films

Sample	$c(\text{Cu}^{2+})$ /(mmol L^{-1})	Resistivity /($\Omega\cdot\text{m}$)	Electrical conductivity /($\text{S}\cdot\text{m}^{-1}$)	Seebeck coefficient /($\mu\text{V}\cdot\text{K}^{-1}$)	Power factor /($\mu\text{W}\cdot\text{K}^{-2}\cdot\text{m}^{-1}$)
1	0.00	1.12×10^{-4}	8.93×10^3	140	175.0
2	0.64	9.86×10^{-5}	1.01×10^4	138	193.1
3	1.28	4.00×10^{-5}	2.50×10^4	152	577.6
4	2.50	7.14×10^{-5}	1.40×10^4	132	244.0
5	3.84	3.08×10^{-5}	3.25×10^4	139	627.3
6	5.00	3.48×10^{-5}	2.87×10^4	134	516.0
7	6.40	3.35×10^{-5}	2.98×10^4	131	512.3
8	7.65	2.25×10^{-5}	4.44×10^4	104	480.7

Power factor is often used to characterize the electrical properties of thermoelectric materials. In order to compare our research with others, the electrical conductivity, Seebeck coefficient as well as the power factor of other reported Cu-doped bismuth telluride materials is listed in Tab.3. It can be seen that the power factor of $\text{Bi}_x\text{Cu}_y\text{Sb}_{2-x-y}\text{Te}_z$ thin film prepared by potentiodynamic deposition in this study is higher than some previously reported Cu-doped bismuth telluride materials.

Table 3. Performance comparison of different Cu doped bismuth telluride based thin film thermoelectric materials

Materials	Electrical conductivity/($\text{S}\cdot\text{m}^{-1}$)	Seebeck coefficient/($\mu\text{V}\cdot\text{K}^{-1}$)	Power factor/($\mu\text{W}\cdot\text{K}^{-2}\cdot\text{m}^{-1}$)	References
$\text{Cu}_x\text{Bi}_2\text{Te}_3$	1.85×10^4	-84	130.7	[33]
Cu-doped Bi_2Te_3	1.17×10^5	63.6	475.5	[34]
Cu-doped Bi_2Te_3	6.00×10^4	-52	160	[35]
Cu-doped Bi_2Te_3	1.00×10^5	-24	57.5	[36]
$\text{Bi}_x\text{Cu}_y\text{Sb}_{2-x-y}\text{Te}_z$	2.50×10^4	152	577.6	this paper

Fig. 3 is the XRD spectrum of the thermoelectric materials doped with and without Cu.

Obvious diffraction peaks at 27.89° , 33.36° , 38.01° , 40.31° , 41.79° , 44.49° , 45.49° , 50.81° , 53.78° , 57.76° , 62.65° and 68.31° can be observed in the XRD pattern of thin film prepared in the electrolyte containing $6.40 \text{ mmol/L Cu}^{2+}$. These diffraction peaks are corresponding to the (015), (018), (1010), (0111), (110), (0015), (116), (024), (0018), (0210), (1019), (125) crystal planes of $\text{Bi}_{0.5}\text{Sb}_{1.5}\text{Te}_3$, respectively. Compared with the XRD pattern of the film deposited in the electrolyte without Cu^{2+} almost no shift of the peak was detected. Similar results can be found in the reported literature.[33, 37] Hu studied the effect of Cu^{2+} concentration on the structure of electrodeposited $\text{Cu}_x\text{Bi}_2\text{Te}_3$ thin films and discovered that as the Cu^{2+} concentration increased, almost no peak shift was observed in the XRD spectra [33]. Han also found that a small amount of Cu doping would not affect the spectral peak characteristics of the Cu-doped Bi_2Te_3 samples [37]. In addition, there is no additional reflection peak associated with copper in the spectrum (Fig.3a), which reveals that Cu element is indeed doped into the structure of the $\text{Bi}_{0.5}\text{Sb}_{1.5}\text{Te}_3$ ternary material rather than deposited in the form of pure Cu. Compared with the XRD spectrum of $\text{Bi}_{0.5}\text{Sb}_{1.5}\text{Te}_3$ material prepared in the electrolyte without Cu^{2+} , it can be clearly seen that the diffraction peaks of Cu-doped material are much sharper and stronger. The results show that doping of Cu element improves the crystallization degree of the material, and further explains the reason why the material doped with Cu can obtain higher thermoelectric properties.

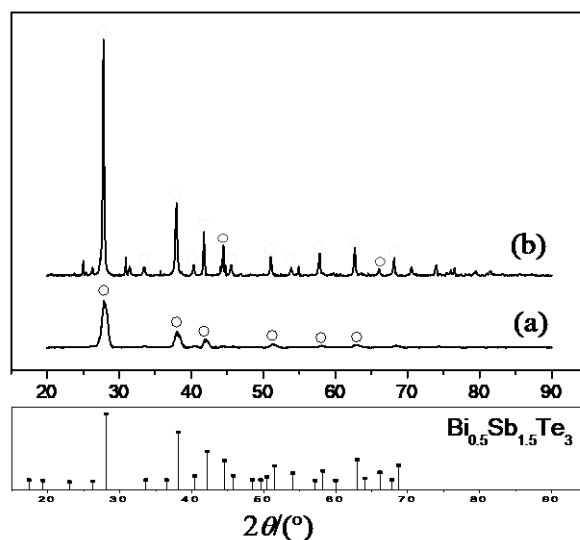


Figure 3. XRD patterns of the films potentiodynamic electrodeposited in the solution containing different concentration of Cu^{2+} (a) $0 \text{ mmol L}^{-1} \text{ Cu}^{2+}$, (b) $6.40 \text{ mmol L}^{-1} \text{ Cu}^{2+}$, $\circ \text{Bi}_{0.5}\text{Sb}_{1.5}\text{Te}_3$ (PDF#49-1713)

3.4 Effect of Cu^{2+} ion concentration on the morphology of $\text{Bi}_x\text{Cu}_y\text{Sb}_{2-x-y}\text{Te}_z$ thin film thermoelectric materials

The morphology of $\text{Bi}_x\text{Cu}_y\text{Sb}_{2-x-y}\text{Te}_z$ thin film thermoelectric materials prepared by potentiodynamic deposition mode in the electrolyte with different Cu^{2+} concentration are shown in Fig.4. It can be seen that with the increase of Cu^{2+} concentration in the solution, the prepared materials become more uniform and dense, and the apparent particle size ranges from $8 \mu\text{m}$ to $2 \mu\text{m}$, which reveals that the morphology of the material is improved. This phenomenon can also be found in Seo's

research, they studied the influence of Cu content on the morphology of Cu-doped Bi_2Te_3 films and detected that Cu-doped Bi_2Te_3 films became gradually dense as a function of Cu content [36], which can be attributed to the fact that the addition of Cu helps to improve the apparent density of the Cu-doped Bi_2Te_3 films.

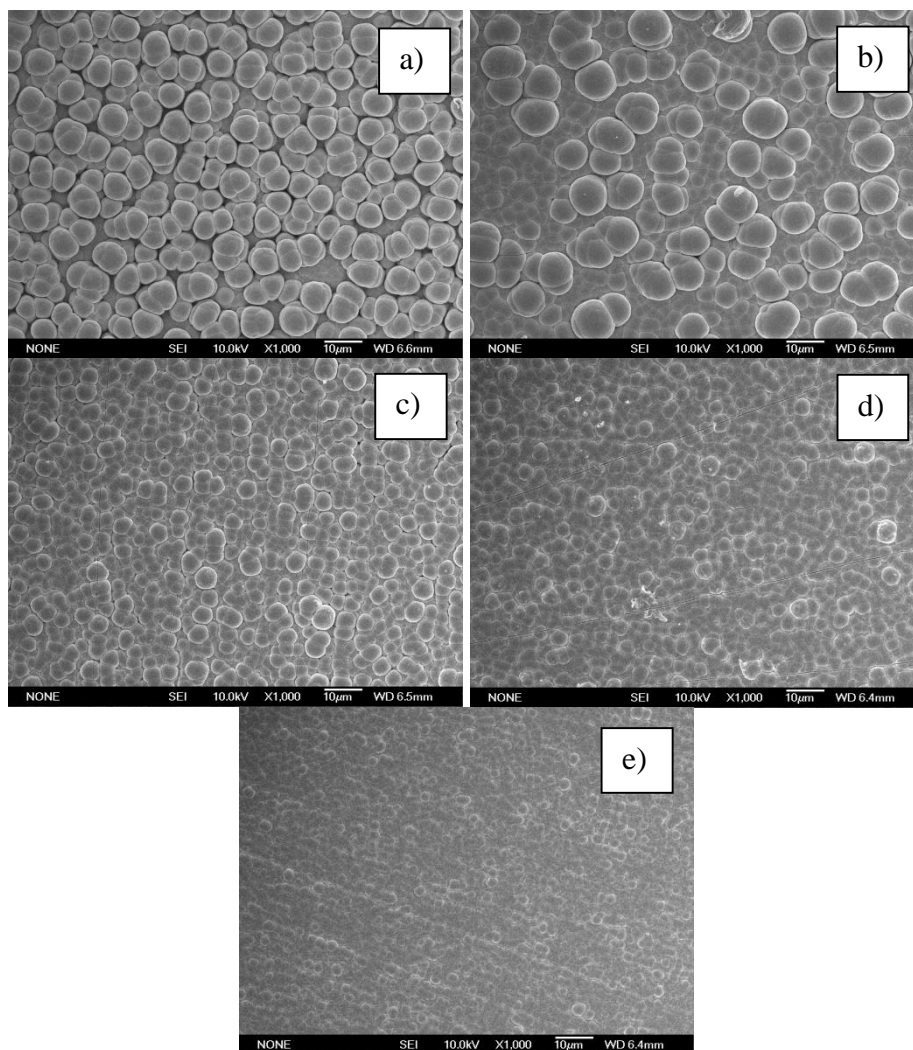


Figure 4. FESEM images of $\text{Bi}_x\text{Cu}_y\text{Sb}_{2-x-y}\text{Te}_z$ thermoelectric films potentialdynamic electrodeposited on Au electrode in the solution containing different concentrations of Cu^{2+} , (a) 2.50 mmol L^{-1} , (b) 3.84 mmol L^{-1} , (c) 5.00 mmol L^{-1} , (d) 6.40 mmol L^{-1} (e) 7.65 mmol L^{-1}

Based on the above results, it can be seen that doping Cu in $\text{Bi}_x\text{Sb}_{2-x}\text{Te}_z$ ternary thermoelectric material can not only reduce the resistivity of the material, but also improve the morphology of the material. In addition, the Seebeck coefficient of $\text{Bi}_x\text{Cu}_y\text{Sb}_{2-x-y}\text{Te}_z$ thermoelectric material obtained by doping Cu can reach up to $152 \mu\text{V/K}$. It can be seen that the doping of Cu can greatly improve the comprehensive properties of the material.

4. CONCLUSIONS

Cu-doped $\text{Bi}_x\text{Cu}_y\text{Sb}_{2-x-y}\text{Te}_z$ thin film thermoelectric materials were prepared on Au substrate by potentiodynamic deposition mode. The effects of Cu^{2+} ion concentration on the morphology, composition, structure and thermoelectric properties of $\text{Bi}_x\text{Cu}_y\text{Sb}_{2-x-y}\text{Te}_z$ thin film thermoelectric materials were investigated. The main conclusions are as follows:

1) In the inorganic solution system, the composition of $\text{Bi}_x\text{Cu}_y\text{Sb}_{2-x-y}\text{Te}_z$ thermoelectric materials prepared by electrodeposition can be changed by changing the concentration of Cu^{2+} in the solution.

2) Doping Cu into $\text{Bi}_x\text{Sb}_{2-x}\text{Te}_z$ ternary thermoelectric material can not only reduce the resistivity of the materials, but also improve the morphology.

3) The Seebeck coefficient and power factor of Cu-doped $\text{Bi}_x\text{Cu}_y\text{Sb}_{2-x-y}\text{Te}_z$ thermoelectric material can reach up to $152 \mu\text{V/K}$ and $577.6 \mu\text{W}\cdot\text{K}^{-2}\cdot\text{m}^{-1}$.

4) Doping of Cu can greatly improve the comprehensive properties of the material.

ACKNOWLEDGEMENT

This work was supported by the Tianjin Municipal Education Committee Project (160020/2016ZT010603).

CONFLICT OF INTEREST STATEMENT

We declare that we do not have any commercial or associative interest that represents a conflict of interest in connection with the work submitted.

References

1. W. Strielkowski, L. Civin, E. Tarkhanova, M. Tvaronaviciene and Y. Petrenko, *Energies*, 14 (2021) 8240.
2. Y.D. Yu, Z.P. Guo, W. Zhu, J. Zhou, S.M. Guo, Y.L. Wang and Y. Deng, *Nano Energy*, 93 (2022) 106818.
3. L.T. Ga, Z. Zhang, D.C. Xu and W.B. Li, *Case Stud. Therm. Eng.*, 28 (2021) 101582.
4. T. Maji, A.M. Rousti, A.P. Kazi, C. Drew, J. Kumar and D.C. Christodouleas, *ACS Appl. Mater. Interfaces*, 13 (2021) 46919.
5. M. Marefati and M. Mehrpooya, *Sustainable Energy Technol. Assess.*, 36 (2019) 100550.
6. Y.F. Chen, F. Wei, H. Wang, W.Y. Zhao and Y. Deng, *Acta Phys. Sin-ch Ed.*, 70 (2021) 207303.
7. J. Recatala-Gomez, P. Kumar, A. Suwardi, A. Abutaha, I. Nandhakumar and K. Hippalgaonkar, *Sci. Rep.*, 10 (2020) 17922.
8. B. Jabar, X.Y. Qin, D. Li, J. Zhang, A. Mansoor, H.X. Xin, C.J. Song and L.L. Huang, *J. Mater. Chem. A*, 7 (2019) 19120.
9. E.M.F. Vieira, J. Figueira, A.L. Pires, J. Grilo, M.F. Silva, A.M. Pereira and L.M. Goncalves, *J. Alloys Compd.*, 774 (2019) 1102.
10. M.R.A. Bhuiyan, H. Mamur and M.F. Dilmac, *Curr. Nanosci.*, 17 (2021) 423.
11. C. J. Vineis, A. Shakouri, A. Majumdar and M.G. Kanatzidis, *Adv. Mater.*, 22 (2010) 3970.
12. J.K. Lee, J.H. Son, Y.I. Kim, B. Ryu, B.J. Cho, S. Kim, S.D. Park and M.W. Oh, *Appl. Sci.-Basel*, 8 (2018) 735.
13. J.L. Cui, H.F. Xue, W.J. Xiu, W. Yang and X.B. Xu, *Scr. Mater.*, 55 (2006) 371.
14. J. Cho, S.I. Kim, Y. Kim, H.S. Kim, T. Park and S.W. Kim, *J. Alloys Compd.*, 884 (2021) 161060.
15. Z.H. Wang, L. Yang, X.J. Li, X.T. Zhao, H.L. Wang, Z.D. Zhang and X.P. Gao, *Nano Lett.*, 14

- (2014) 6510.
16. H. Wu, P. Zhang, P. Deng, Q. Lan, Q. Pan, S.A. Razavi, X. Che, L. Huang, B. Dai, K. Wong, X. Han and K.L. Wang, *Phys. Rev. Lett.*, 123 (2019) 207205.
 17. D. Rosenbach, N. Oellers, A.R. Jalil, M. Mikulics, J. Kölzer, E. Zimmermann, G. Mussler, S. Bunte, D. Grützmacher, H. Lüth and T. Schäpers, *Adv. Electron. Mater.*, 6 (2020) 2000205.
 18. Z. Liao, M. Brahlek, J.M. Ok, L. Nuckols, Y. Sharma, Q. Lu, Y. Zhang and H.N. Lee, *APL Mater.*, 7 (2019) 041101.
 19. S.X. Zhang, R.D. McDonald, A. Shekhter, Z.X. Bi, Y. Li, Q.X. Jia and S.T. Picraux, *Appl. Phys. Lett.*, 101 (2012) 202403.
 20. P. Fan, P.C. Zhang, G.X. Liang, F. Li, Y.X. Chen, J.T. Luo, X.H. Zhang, S. Chen and Z.H. Zheng, *J. Alloys Compd.*, 819 (2020) 153027.
 21. N. Theekhasuk, R. Sakdanuphab, P. Nuthongkum, P. Pluengphon, A. Harnwunggmoung, M. Horprathum, P. Limsuwan, A. Sakulalavek and P. Sukwisute, *Curr. Appl Phys.*, 31 (2021) 7-15.
 22. R. Eguchi, H. Yamamuro and M. Takashiri, *Thin Solid Films*, 714 (2020) 138356.
 23. R. Rani, S. Tusseau-Nenez, P.E. Coulon, T.L. Wade and M. Konczykowski, *Iscience*, 24 (2021) 102694.
 24. F.H. Li and W. Wang, *Electrochim. Acta*, 55 (2010) 5000.
 25. T.J. Wu, J. Kim, J.H. Lim, M.S. Kim and N.V. Myung, *Front. Chem.*, 9 (2021) 762896.
 26. M. Martín-González, G.J. Snyder, A.L. Prieto, R. Gronsky and A.M. Stacy, *Nano Lett.*, 2003, 3(7): 973-977.
 27. D.D. Frari, S. Diliberto, N. Stein, C. Boulanger and J.M. Lecuire, *Thin Solid Films*, 483 (2005) 44.
 28. D.D. Frari, S. Diliberto, N. Stein, C. Boulanger and J.M. Lecuire, *J. Appl. Electrochem.*, 36 (2006) 449.
 29. V. Richoux, S. Diliberto, C. Boulanger and J.M. Lecuire, *Electrochim. Acta*, 52 (2007) 3053.
 30. S. Diliberto, V. Richoux, N. Stein and C. Boulanger, *Phys. Status Solidi A*, 205 (2008) 2340.
 31. T. J. Yoon, Y. H. Park and T. S. Oh, *Mater. Sci. Forum.*, 544-545 (2007) 917.
 32. F.H. Li, Q.H. Huang and W. Wang, *Electrochim. Acta*, 54 (2009) 3745.
 33. Y.C. Hu, Z.G. Zou and K.F. Cai, *Mater. Sci. Forum*, 787 (2014) 205.
 34. B.G. Kim, S.H. Bae, J. Byeon, C. Lee and S. Choi, *Mater. Lett.*, 270 (2020) 127697.
 35. B.G. Kim, K.H. Seo, C.H. Lim and S.M. Choi, *J. Mater. Res. Technol.*, 15 (2021) 606.
 36. K.H. Seo, B.G. Kim, C.H. Lim, S.H. Kim, K.M. Lee, J.Y. Kim and S.M. Choi, *Crystengcomm*, 19 (2017) 2750.
 37. Y. Han, M. Li, Z. Zhang, S. Jiang, J. Liu, Y. Liu, W. Li and J. Liu, *Mater. Sci.*, 11 (2021) 350.